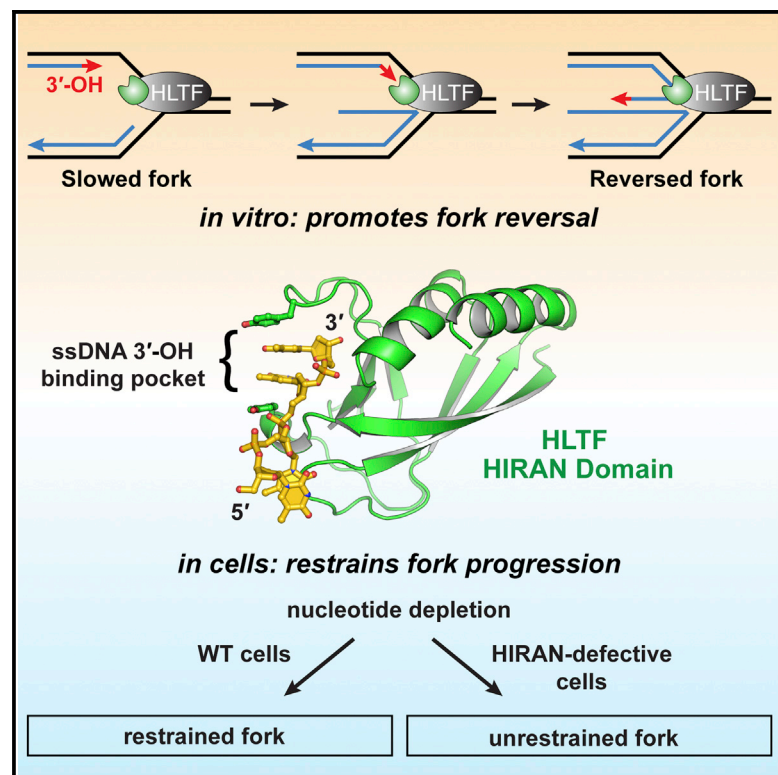


# Molecular Cell

## HLTF's Ancient HIRAN Domain Binds 3' DNA Ends to Drive Replication Fork Reversal

### Graphical Abstract



### Authors

Andrew C. Kile, Diana A. Chavez, Julien Bacal, ..., Irina Bezsonova, Brandt F. Eichman, Karlene A. Cimprich

### Correspondence

brandt.eichman@vanderbilt.edu (B.F.E.), cimprich@stanford.edu (K.A.C.)

### In Brief

Kile et al. reveal the function and structure of the ancient and evolutionarily conserved HIRAN domain of HLTF, a dsDNA translocase involved in replication fork reversal. They show it to be a recognition module for 3' DNA ends necessary for fork reversal in vitro and also for fork progression in vivo.

### Highlights

- The ancient, conserved HIRAN domain is an ssDNA 3' end recognition module
- X-ray and NMR analysis of HIRAN-ssDNA reveal the structural basis for 3' binding
- Fork reversal by HLTF requires HIRAN and the 3' end of the nascent leading strand
- HLTF restrains fork progression under conditions of nucleotide depletion

### Accession Numbers

4S0N  
2MZN



# HLTF's Ancient HIRAN Domain Binds 3' DNA Ends to Drive Replication Fork Reversal

Andrew C. Kile,<sup>1</sup> Diana A. Chavez,<sup>2</sup> Julien Bacal,<sup>1</sup> Sherif Eldirany,<sup>3</sup> Dmitry M. Korzhnev,<sup>3</sup> Irina Bezsonova,<sup>3</sup> Brandt F. Eichman,<sup>2,\*</sup> and Karlene A. Cimprich<sup>1,\*</sup>

<sup>1</sup>Department of Chemical and Systems Biology, Stanford University School of Medicine, Stanford, CA 94305, USA

<sup>2</sup>Department of Biological Sciences and Center for Structural Biology, Vanderbilt University, Nashville, TN 37232, USA

<sup>3</sup>Department of Molecular Biology and Biophysics, University of Connecticut Health Center, Farmington, CT 06032, USA

\*Correspondence: [brandt.eichman@vanderbilt.edu](mailto:brandt.eichman@vanderbilt.edu) (B.F.E.), [cimprich@stanford.edu](mailto:cimprich@stanford.edu) (K.A.C.)

<http://dx.doi.org/10.1016/j.molcel.2015.05.013>

## SUMMARY

Stalled replication forks are a critical problem for the cell because they can lead to complex genome rearrangements that underlie cell death and disease. Processes such as DNA damage tolerance and replication fork reversal protect stalled forks from these events. A central mediator of these DNA damage responses in humans is the Rad5-related DNA translocase, HLTF. Here, we present biochemical and structural evidence that the HIRAN domain, an ancient and conserved domain found in HLTF and other DNA processing proteins, is a modified oligonucleotide/oligosaccharide (OB) fold that binds to 3' ssDNA ends. We demonstrate that the HIRAN domain promotes HLTF-dependent fork reversal *in vitro* through its interaction with 3' ssDNA ends found at forks. Finally, we show that HLTF restrains replication fork progression in cells in a HIRAN-dependent manner. These findings establish a mechanism of HLTF-mediated fork reversal and provide insight into the requirement for distinct fork remodeling activities in the cell.

## INTRODUCTION

Stalled replication forks and other downstream effects of replication stress are significant challenges to genome stability. Unrepaired DNA damage, secondary DNA structures, protein-DNA complexes, and nucleotide depletion can all lead to replication fork collapse and DNA breaks, and eventually to cell death and disease (Branzei and Foiani, 2010; Ciccio and Elledge, 2010; Zeman and Cimprich, 2014). Cells therefore have developed a number of mechanisms to respond to replication stress, bypass stalled replication forks, and repair damaged DNA. DNA damage tolerance (DDT) pathways, for example, minimize fork stalling through bypass of replication blocks and leave resolution of the block for a later time (Branzei and Foiani, 2010; Saugar et al., 2014). In one form of DDT, translesion synthesis polymerases directly bypass lesions in what can be an error-prone process. In another form of DDT, an alternative template is used

(template switching) to enable error-free bypass. Understanding the molecular pathways controlling these processes is key to understanding how cells maintain genomic integrity in the face of replication stress, and how errors in DNA damage response pathways lead to diseases such as cancer.

One versatile mechanism for overcoming stalled replication forks is fork reversal (also called fork regression). Fork reversal involves active remodeling of the stalled replication fork, in which the three-armed fork is converted into a Holliday junction (HJ)-like structure by pairing the newly synthesized sister chromatids to form a fourth regressed arm. This structural change can have several protective effects on genomic integrity (Neelsen and Lopes, 2015). For example, fork reversal minimizes ssDNA formation resulting from polymerase stalling, thus stabilizing the replication fork. Fork reversal also repositions fork-stalling lesions in the context of dsDNA, facilitating DNA repair. Lastly, fork reversal creates an opportunity for template switching. This final process allows the indirect and error-free bypass of fork-blocking lesions using the undamaged sister chromatid. Genotoxic agents, repetitive DNA sequences, and oncogene-induced replication stress all lead to fork regression in mammalian cells, suggesting this process may be a common response to stalled forks (Follonier et al., 2013; Neelsen et al., 2013; Zellweger et al., 2015). Despite growing evidence for the importance of fork reversal in protecting the genome, and what may be the frequent use of this process in fork repair, how fork reversal occurs is not well understood.

Recent evidence suggests that molecular components of DDT might be involved in fork reversal. In yeast, error-free DDT is dependent on Rad5, a RING domain-containing ubiquitin ligase, which promotes the polyubiquitination of proliferating cell nuclear antigen (PCNA) (Hoegel et al., 2002). In mammalian cells, two Rad5-related proteins, SHPRH and HLTF, promote PCNA polyubiquitination (Motegi et al., 2006, 2008; Saugar et al., 2014; Unk et al., 2006, 2008). This modification has been hypothesized to recruit other factors to the stalled fork that promote a template switch (Saugar et al., 2014). Several lines of evidence suggest that DDT proteins might also affect template switching directly by fork remodeling. Rad5, HLTF, and SHPRH are all members of the SWI/SNF2 family of ATP-dependent DNA translocases involved in chromatin remodeling and DNA repair (Unk et al., 2010). Moreover, the ability of Rad5 and HLTF to promote replication of damaged DNA requires both their ubiquitin ligase and DNA translocase domains (Blastyák et al., 2010; Choi

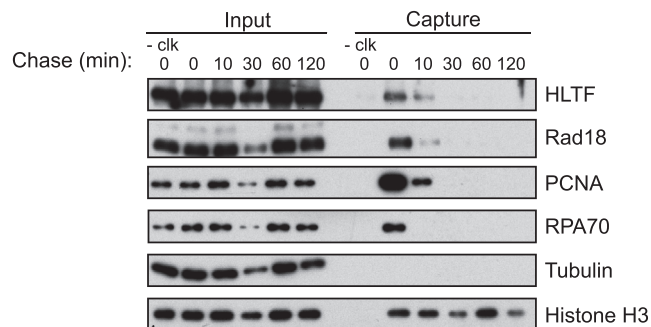


**Figure 1. HLTF and RAD18 Are Enriched at the Replication Fork**

293T cells were pulsed with EdU for 10 min and chased with thymidine for the time shown. Cells were then fixed with 1% formaldehyde and collected. Nascent DNA-protein complexes were purified by iPOND, and EdU-associated proteins were analyzed by western blotting. The -clk condition represents cells pulsed with EdU, and processed without biotin-azide in the click reaction step.

et al., 2015; Gangavarapu et al., 2006; Minca and Kowalski, 2010; Ortiz-Bazán et al., 2014). Indeed, HLTF and Rad5 can directly catalyze replication fork reversal on model DNA substrates (Achar et al., 2011; Blastyák et al., 2007, 2010). Interestingly, HLTF and Rad5 lack the strand unwinding activity associated with canonical helicases, and instead use their dsDNA translocase activity to promote fork reversal and branch migration in an ATP-dependent manner (Achar et al., 2011; Blastyák et al., 2007, 2010). In spite of these observations, it is not known whether or how Rad5-related proteins mediate fork reversal in cells following replication stress.

Structural elements within Rad5-related proteins provide intriguing clues about their potential mechanism of action in fork reversal. Rad5, HLTF, and SHPRH share a domain structure that contains a ubiquitin ligase RING motif embedded within the SWI2/SNF2 ATPase motor (Unk et al., 2010). In addition, HLTF and Rad5 contain an uncharacterized HIP116/HLTF Rad5 N terminus (HIRAN) domain, which has been proposed to bind damaged DNA structures such as those found at stalled replication forks (Iyer et al., 2006). The HIRAN domain is ancient and highly conserved among organisms from bacteria to humans. In prokaryotes, it is often found in proteins with no other identifiable motifs. In eukaryotes, it is often coupled to DNA-processing domains, including tyrosyl-DNA phosphodiesterase and viral replication and repair (VRR) nuclease domains, suggesting that the HIRAN domain may be integral to the function of these proteins. Consistent with this idea, deletion of the HIRAN domain in the *S. pombe* ortholog of Rad5 leads to DNA damage sensitivity (Ding and Forsburg, 2014).

In this study, we describe an important role for the HIRAN domain in driving replication fork regression by HLTF. Using biochemical, structural, and genetic approaches, we establish that the HIRAN domain recognizes 3' ssDNA ends and directs HLTF to the 3' end of the nascent leading strand to remodel replication forks. This requirement for the 3' end is unique among factors involved in replication fork reversal, and the 3' end binding activity appears to be a conserved activity of the ancient HIRAN domain. Lastly, we demonstrate this activity is required for fork

progression in cells by showing that the 3' end-binding function of HIRAN affects the length of newly synthesized DNA fibers. Our findings indicate that the HIRAN domain is a substrate specificity factor for HLTF that dictates its biological activity, and thus provide important insights into the distinct mechanism by which HLTF recognizes and remodels replication forks.

## RESULTS

### HLTF Associates with the Replication Fork

Fork reversal by HLTF, if relevant in vivo, would be expected to occur on chromatin and at the replication fork. To determine whether HLTF is present at active replisomes, we used iPOND (isolation of proteins on nascent DNA) (Sirbu et al., 2011) to capture nascent, EdU-labeled DNA and its associated proteins from proliferating cells. We found that HLTF is associated with EdU-labeled DNA immediately after the EdU pulse, but not 10–30 min after the EdU was washed out (Figure 1). RAD18, a RING domain-containing protein that interacts with HLTF (Motegi et al., 2008; Unk et al., 2008), also associated with nascent EdU-labeled DNA with similar kinetics, as did RPA and PCNA, two well-established markers of the replication fork. Together, these findings demonstrate that HLTF is a component of active replisomes, but not mature chromatin. Furthermore, they suggest that HLTF associates with DNA at a replication fork, even in the absence of exogenous DNA damage or replication stress.

### The HIRAN Domain Binds the 3' End of ssDNA

HLTF binds and remodels various forked DNA structures, although the manner in which it recognizes these DNA structures is not known (Blastyák et al., 2010). We were intrigued by the possibility that the evolutionarily conserved (Figure 2A; Figure S1), yet functionally uncharacterized N-terminal HIRAN domain of HLTF is important for its DNA recognition and remodeling activities. To investigate its potential DNA-binding ability, we purified the HIRAN domain (residues 55–180) of human HLTF and examined its interaction with single- or double-stranded DNA (ssDNA, dsDNA) oligonucleotides using electrophoretic mobility shift assays (EMSA). Surprisingly, we found that the HIRAN domain had a strong affinity for ssDNA ( $K_d = 13 \pm 3$  nM), but showed no detectable affinity for dsDNA (Figure 2B). In contrast, binding of the HLTF HIRAN domain to short dsDNA oligonucleotides containing blunt and recessed 3' ends was recently reported (Hishiki et al., 2015). However, since the duplex regions in those experiments contained only 8–13 nucleotides, the possibility of duplex denaturation cannot be ruled out.

To further explore how the HIRAN domain directs HLTF to ssDNA, we immobilized single-stranded 20-mer oligonucleotides modified with biotin at either the 3' or 5' end on streptavidin beads and tested binding to these complexes. Consistent with our EMSA results, the isolated HIRAN domain bound to ssDNA. Unexpectedly, however, HIRAN exhibited a strong preference for the ssDNA oligonucleotide that was immobilized via the 5' end and had a free 3' hydroxyl group (Figure 2C). Importantly, purified full-length HLTF exhibited the same binding specificity to ssDNA, indicating that apparent 3' ssDNA end binding activity is a property of full-length HLTF, and not just the HIRAN domain.

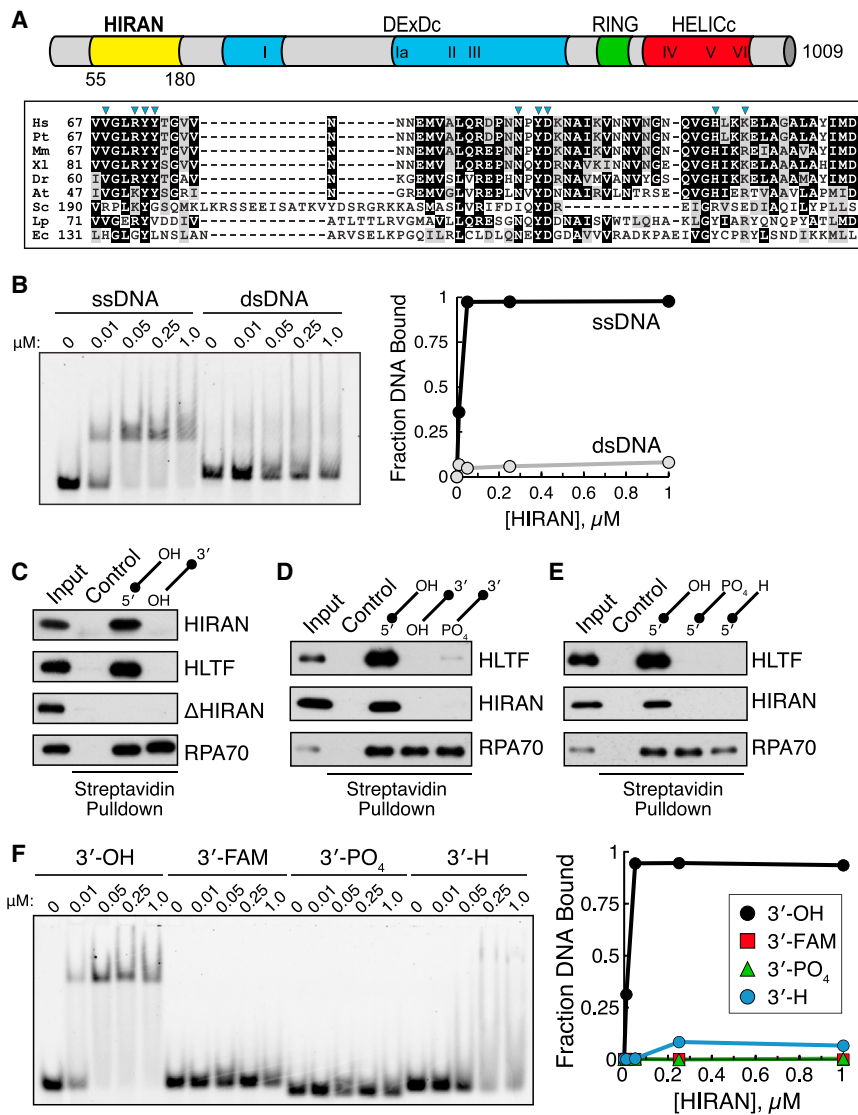


**Figure 2. The HLTF-HIRAN Domain Binds the 3' End of ssDNA**

(A) Domain schematic of HLTF. The sequence alignment shows conservation within HIRAN domains from seven eukaryotic HLTF orthologs and two bacterial proteins of unknown function. Hs, *Homo sapiens*; Pt, *Pan troglodytes*; Mm, *Mus musculus*; Xl, *Xenopus laevis*; Dr, *Danio rerio*; At, *Arabidopsis thaliana*; Sc, *Saccharomyces cerevisiae*; Lp, *Lactobacillus plantarum*; Ec, *Escherichia coli*. Arrows above the alignment indicate conserved residues that contact DNA (see Figure 4; Figure S1).

(B) EMSA of HIRAN binding to 5'-FAM-labeled 40-mer ssDNA and dsDNA. Quantitation of the gel is shown on the right.

(C–E) Capture of purified proteins by biotinylated 20-mer ssDNA. The biotin position at the 5' or 3' end is indicated by the ● symbol. Control, no DNA. (F) EMSA of HIRAN binding to 5'-FAM-labeled dT<sub>10</sub> oligonucleotides modified as shown at the 3' end. Quantitation of the gel is shown on the right.

fied at their 3' ends yielded similar results (Figure 2F). Taken together, these observations establish that the HIRAN domain interacts with ssDNA 3' ends via the 3'-hydroxyl group.

### Structural Basis for 3' End Binding by the HIRAN Domain

To elucidate the molecular details of HLTF's DNA binding specificity, we determined an X-ray crystal structure of the HIRAN domain bound to ssDNA (Figure 3A; Figure S2A). We refined a model containing four protein-DNA complexes in the asymmetric unit (asu) against data extending to 1.5-Å resolution to a crystallographic residual (R/R<sub>free</sub>) of 15.2%/18.4% (Table 1). In each complex in the

Moreover, deletion of the HIRAN domain from the full-length protein ( $\Delta$ HIRAN) completely abolished the interaction of HLTF with ssDNA, demonstrating that the HIRAN domain is both necessary and sufficient for the ssDNA binding activity of HLTF (Figure 2C). Another ssDNA binding protein, RPA, showed no preference for binding to either oligonucleotide, a finding that highlights the specificity of this interaction and also indicates that there are equal amounts of DNA in the pull-downs (Figure 2C). Neither HLTF nor the HIRAN domain bound 5'-phosphorylated ssDNA, suggesting the lack of binding is not due to lack of a phosphate group naturally found at the 5' ends of DNA (Figure 2D). Next, we investigated the specificity of the HIRAN domain for a 3' end by monitoring binding of HLTF and the HIRAN domain to ssDNA containing a hydroxyl (-OH), phosphate (-PO<sub>4</sub>), or hydrogen (-H) at the 3' position (Figure 2E). Both HLTF and the HIRAN domain failed to bind ssDNA oligonucleotides that were modified at the 3' end, whereas RPA binding was not disrupted (Figure 2E). EMSA experiments with dT<sub>10</sub> oligonucleotides modi-

asu, all 125 HIRAN residues and at least four nucleotides at the 3' end of each DNA strand were resolved. Our model revealed that the HIRAN domain adopts a globular  $\alpha$ + $\beta$  architecture with an embedded oligonucleotide/oligosaccharide binding (OB)-fold ( $\beta$ 2– $\beta$ 6)—a general nucleic acid-binding platform (Theobald et al., 2003) (Figure 3A). Two loops between  $\beta$ 1 and  $\beta$ 2 (L<sub>12</sub>) and  $\beta$ 2 and  $\beta$ 3 (L<sub>23</sub>) extend from the OB-fold and with the  $\beta$ 2– $\beta$ 3– $\beta$ 4/ $\alpha$ B surface form a binding pocket for the 3' end of ssDNA. In each of the four complexes in the asu, the two nucleotides at the 3' ends are well ordered inside this pocket. The 5' ends of the DNA are directed away from the protein surface by a loop between  $\beta$ 5 and  $\beta$ 6 (L<sub>56</sub>) and participate in crystal contacts with neighboring protein molecules. As a consequence, the conformations of the 5' ends are highly variable (Figure S2B).

Comparison to other structures in the Protein Databank (PDB) revealed that the HLTF HIRAN domain is virtually identical to that of a predicted HIRAN domain within a protein of unknown function from *Lactobacillus plantarum* (PDB: 3K2Y; Figure S2C). This

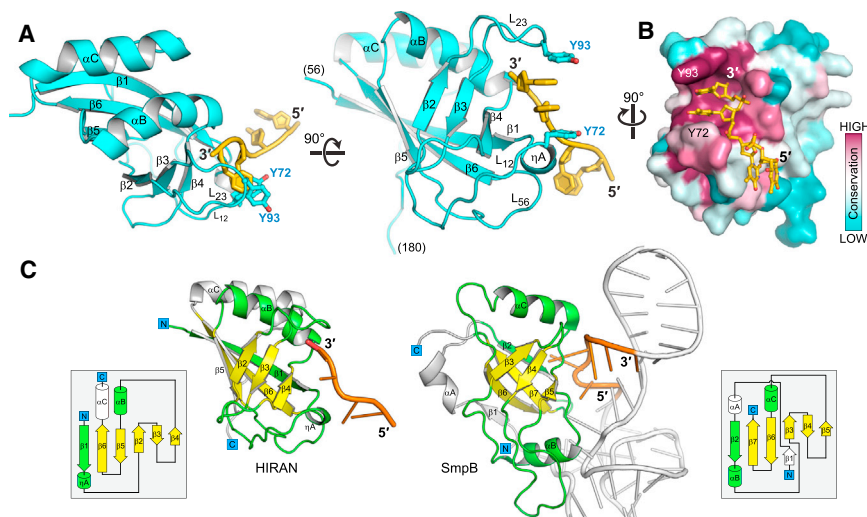


**Figure 3. Structure of the HLTf-HIRAN Domain Bound to ssDNA**

(A) The crystal structure of the HLTf HIRAN domain bound to dT<sub>10</sub> ssDNA (gold).

(B) Sequence conservation from 150 HIRAN orthologs mapped onto the solvent accessible surface of the HIRAN crystal structure using the ConSurf web server (<http://consurf.tau.ac.il>).

(C) Comparison of HLTf HIRAN-ssDNA and SmpB-tRNA (PDB: 2CZJ) structures. Homologous protein secondary structural elements are shown in green, OB-folds in yellow, and nucleic acid segments contacting the OB-fold in orange. Topology diagrams are shown below and are colored according to the structures. See also Figure S2.

similarity indicates that the HIRAN fold is conserved in organisms separated by more than a billion years of evolution. The 3'-binding pocket in HIRAN is also strongly conserved, as indicated by mapping sequence homology of HIRAN domains from 150 proteins onto the crystal structure (Figure 3B). We also found that the HIRAN domain shares significant structural homology with small protein B (SmpB, PDB: 2CZJ), the tRNA-binding component of the bacterial transfer mRNA machinery (Bessho et al., 2007; Dong et al., 2002) (Figure 3C). Interestingly, SmpB binds an internal segment of RNA using the same general surface that HIRAN uses to bind ssDNA (Bessho et al., 2007), although the specific HIRAN-DNA and SmpB-RNA contacts are distinct. Similarly, the 3' end binding of the HIRAN OB-fold is distinctly different than the manner in which RPA's OB folds bind ssDNA (Theobald et al., 2003).

Upon comparing the HIRAN architecture to other known 3' end-binding domains, we found structural similarity to nucleic acid-binding proteins from organisms throughout evolution, ranging from the 3' DNA-binding domain (3'BD) of the bacterial PriA replication restart helicase to the 3' RNA-binding PAZ domain of human Argonaute-1 (Ma et al., 2004; Sasaki et al., 2007). Each of these end-binding domains uses a topologically distinct arrangement of  $\beta$  strands to achieve a similar 3D architecture. Indeed, superposition of these structures places the nucleic acid binding surfaces in the same location relative to the  $\beta$  sheet motifs (Figure S2D). Thus, the HIRAN fold represents a general nucleic acid binding architecture that HLTf and other proteins have adapted to bind specifically to 3' ends. We note that not all 3'-binding domains show this same architecture. For example, Flap endonuclease-1 (FEN-1) captures the 3' end at a DNA nick using an  $\alpha$ -helical domain with no structural resemblance to HIRAN, PriA-3'BD, or PAZ domains (Tsutakawa et al., 2011).

### DNA Binding by the HIRAN Domain Is Confined to the 3'-Binding Pocket

Analysis of our crystal structure revealed several interactions that form the basis for HIRAN's specificity for 3' ends. First, the

DNA 3'-hydroxyl group is nestled deep in the back of the pocket and hydrogen bonded to the carboxyl side chain of D94 (Figure 4A), explaining the requirement for a free 3'-hydroxyl for binding. Second, two nucleobases at the 3' end are stacked between two tyrosine side chains (Y72 and Y93) that extend from loops L<sub>12</sub> and L<sub>23</sub>, and the Watson-Crick faces of these two nucleobases are hydrogen bonded to Y73, N91, and H110. These interactions preclude binding of dsDNA inside this pocket. Consistent with this, a recently published crystal structure of HIRAN with dsDNA (PDB: 4XZF) showed the domain bound to two unduplexed nucleotides at the 3' end, in a manner virtually identical to our structure (RMSD = 0.51 Å for all atoms) (Hishiki et al., 2015). Lastly, the phosphates of the two 3'-nucleotides are stabilized by electrostatic interactions with R71 and K113 side chains as well as a hydrogen bond from the Y72 hydroxyl group. Outside of the binding pocket, the third nucleotide from the 3' end is base-stacked against F142 from loop L<sub>56</sub>, placing a 90° kink in the trajectory of the ssDNA. Thus, the two nucleotides at the 3' end are stabilized by an extensive network of interactions, and we observe no binding outside of the 3' pocket. Notably, all of the residues in the DNA binding pocket are conserved in the *Lactobacillus* lp\_0118 protein, with the exception of H110, which in lp\_0118 is a tyrosine capable of analogous hydrogen bonding with the DNA bases. This striking conservation indicates that 3' binding is conserved in the bacterial HIRAN proteins.

To investigate the full extent of the DNA binding interface in the absence of crystal lattice contacts that might bias binding of the DNA outside of the 3'-binding pocket, we monitored DNA binding in solution using nuclear magnetic resonance (NMR) chemical shift perturbation. The <sup>15</sup>N-HSQC spectra of the free HIRAN domain showed chemical shift dispersion indicative of folded protein (Figure S3A). Upon addition of ssDNA, peak broadening diminished, and a number of additional strong peaks appeared (Figure 4B; Figure S3A), indicating that ssDNA binding stabilizes flexible regions of the protein. The addition of dsDNA had no effect on the NMR spectrum, consistent with our finding that HIRAN did not bind dsDNA.

**Table 1. HIRAN-ssDNA X-Ray Data Collection and Refinement Statistics**

	Native	SeMet
Data Collection <sup>a</sup>		
Space group	P2 <sub>1</sub>	P2 <sub>1</sub>
Cell Dimensions		
a, b, c (Å)	61.03, 74.21, 66.18	60.87, 74.28, 65.93
α, β, γ (°)	90.00, 113.68, 90.00	90.00, 113.76, 90.00
Wavelength	0.97872	0.97872
Resolution (Å)	100–1.50 (1.55–1.50)	100–1.92 (1.99–1.92)
R <sub>sym</sub>	0.068 (0.455)	0.097 (0.507)
I/σI	27.2 (3.9)	20.3 (4.3)
Completeness (%)	99.8 (100)	100 (100)
Redundancy	7.6 (7.5)	7.6 (7.6)
Refinement		
Resolution (Å)	1.5	
No. reflections	86,121	
R <sub>work</sub> /R <sub>free</sub>	0.1528/0.1849	
No. atoms	4,933	
Protein/DNA	3,939/389	
Solvent	605	
B-Factors		
Protein/DNA	32.4/48.9	
Solvent	39.7	
Rms Deviations		
Bond lengths (Å)	0.006	
Bond angles (°)	0.973	

<sup>a</sup>Numbers in parentheses refer to data in the highest-resolution shell.

Next, we monitored chemical shift changes ( $\Delta\omega$ ) for each residue in the <sup>15</sup>N-HSQC spectrum upon addition of ssDNA (Figure 4C) and mapped these onto the surface of the HIRAN crystal structure (Figure 4D). We observed the largest chemical shift changes within strand  $\beta$ 4 and loops L<sub>12</sub>, L<sub>23</sub>, and L<sub>56</sub>, consistent with the crystal structure. Thus, ssDNA does not appear to significantly interact with the surface of the protein outside of the 3'-binding pocket. Lastly, we determined the solution structure of the DNA-bound form of HIRAN and found it to be consistent with the X-ray structure, with an RMSD of 1.47 Å for all backbone atoms (PDB: 2MZN; Table S2; Figure S3B). Thus, multiple techniques demonstrate that the HIRAN domain engages a 3' end of ssDNA using a highly conserved network of residues.

To investigate the functional importance of residues mediating the interaction between HIRAN and the 3' end of ssDNA, we purified and tested mutant HIRAN domains containing substitutions at each of the residues identified above for their ability to bind ssDNA by EMSA (Figures 4E and S3C). None of the substitutions significantly destabilized the protein, as determined by thermal denaturation profiles (Figure S3D). They did significantly reduce DNA binding, however. Substitution of R71 with glutamate had the most dramatic effect on ssDNA binding: under two different experimental conditions, R71E led to either 80% reduction (Figures 4E–4G; Figures S3E and S3F) or complete abrogation (Figure S3F) of specific binding for all protein concen-

trations tested. K113E, N91A, D94A, and H110A mutants decreased ssDNA binding affinity by three orders of magnitude (Figures 4F and 4G). Substitution of base-stacking residues had a more modest effect, reducing binding by 60-fold (Y72A Y93A double mutant) and 15-fold (F142A mutant) (Figures 4E–4G). These results indicate that all residues lining the DNA binding pocket are critical for HIRAN binding to DNA, and that at least in our experimental conditions, the polar contacts to the phosphoribose backbone and nucleobases contribute more to the strength of the interaction than do the base-stacking interactions.

### HLTF Fork Reversal Activity Requires a Functional HIRAN Domain

The interaction of the HIRAN domain with ssDNA raised the possibility that this domain might facilitate HLTF-catalyzed DNA remodeling by directing its translocase activity to specific substrates in vivo. Indeed, throughout evolution HIRAN has often appeared in ATPase motor-containing proteins. To test whether 3' end binding by the HIRAN domain is required for HLTF's known activities, we purified a panel of full-length HLTF proteins with single mutations of the residues we found to compromise the HIRAN-ssDNA interaction. We also purified a D557A/E558A (DEAA) Walker B mutant previously shown to lack ATPase and fork regression activity (Blastyák et al., 2010; Gangavarapu et al., 2006) (Figure S4). In contrast to the DEAA mutant, all of the HIRAN mutants were proficient in DNA-dependent ATPase activity (Figure 5A), indicating that DNA binding by HIRAN is not required for HLTF's ATPase activity, and that the HIRAN mutations do not noticeably disrupt the functional integrity of HLTF. Next, we asked whether mutating the HIRAN domain affected the ability of HLTF to catalyze fork regression on a model fork structure. Strikingly, the HIRAN mutants had a reduced ability to reverse a model replication fork (Figure 5B). The R71E and the Y72A/Y93A mutations caused the greatest defects in fork regression, whereas the D94A or H110A mutations had more moderate effects. Together, these data indicate that DNA binding by the HIRAN domain is important for HLTF's fork regression activity through a mechanism other than impairment of ATP hydrolysis.

### 3' DNA Ends Uniquely Promote HLTF-Dependent Fork Regression

Stalled replication forks contain a 3'-hydroxyl group on the nascent leading strand, and the requirement for the HIRAN domain in HLTF-mediated fork regression suggested that this group might be required for HLTF to promote fork regression. To test this hypothesis, we compared HLTF's ability to regress model replication forks containing either an unmodified (3'-OH) or phosphorylated (3'-PO<sub>4</sub>) 3' end on the nascent leading strand. Indeed, we found that HLTF had reduced activity toward the 3'-PO<sub>4</sub>-capped fork, although this defect could be overcome at significantly higher concentrations of HLTF (Figure 6A; Figure S5A).

A number of mammalian enzymes other than HLTF can also catalyze fork reversal in vitro, including SMARCAL1 (Bétous et al., 2012; Ciccina et al., 2012). To determine if SMARCAL1 is similarly affected by the 3'-PO<sub>4</sub>-capped fork structure, we tested

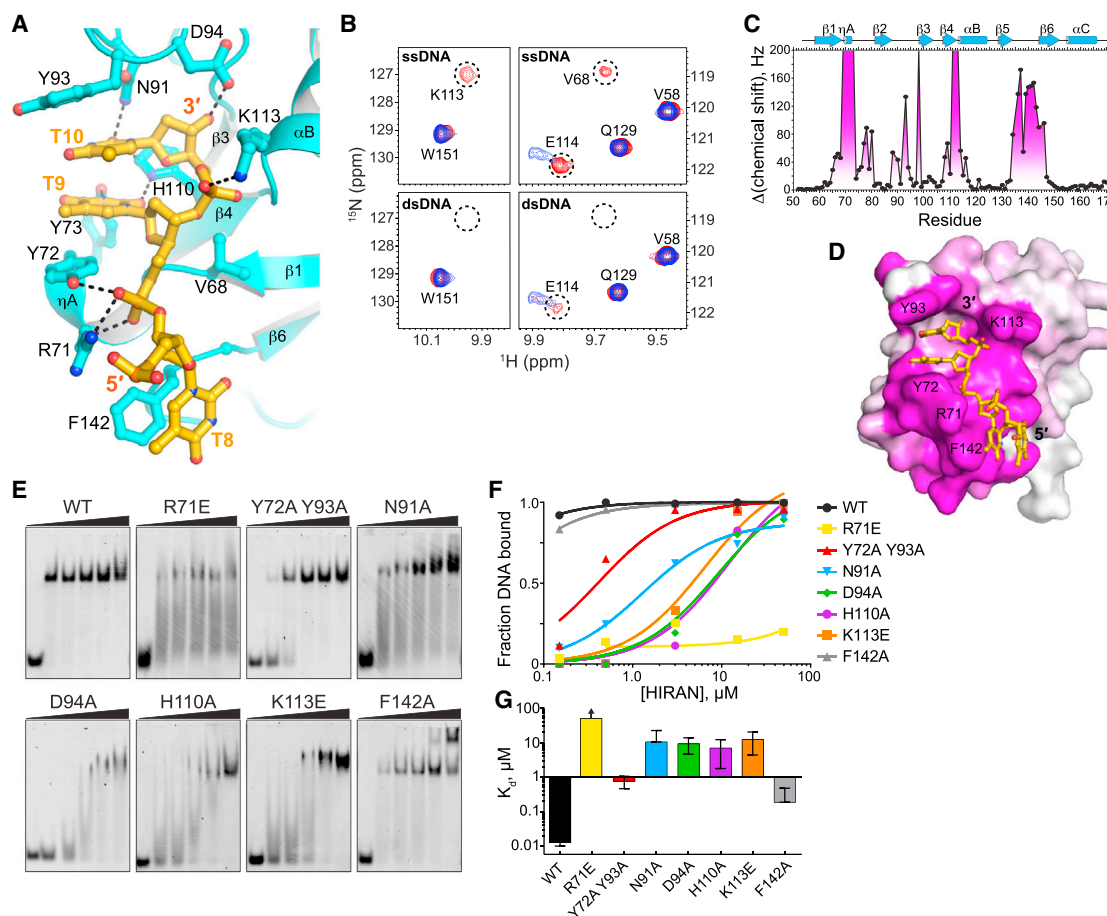


**Figure 4. HIRAN Residues Responsible for DNA Binding**

(A) Details of the HIRAN-DNA interactions observed in the crystal structure. Hydrogen bonds are shown as dashed lines.

(B) NMR chemical shift perturbation of  $^{15}\text{N}$ -labeled HIRAN in the absence (blue) and presence (red) of ssDNA (top) or dsDNA (bottom). The full  $^1\text{H}$ - $^{15}\text{N}$  HSQC spectra are shown in Figure S3A. In the absence of DNA, residue E114 gives rise to multiple weak NMR resonances that collapse into a single strong peak in the DNA-bound state. Similarly, the amide peaks of V68 and K113 are only observed in the spectrum of the HIRAN-ssDNA complex.

(C) NMR chemical shift changes plotted by protein residue number. Resonances that were not detected in the free protein but appeared in the complex were arbitrarily set to  $> 200$  Hz.

(D) HIRAN solvent accessible surface colored according to NMR chemical shift perturbation from (C), with the degree of magenta representing increased chemical shift changes in response to dT<sub>10</sub> binding.

(E) EMSA of FAM-ssDNA in the presence of increasing concentrations of wild-type (WT) and mutant HIRAN proteins. Concentrations of protein were chosen to show the full range of binding for all mutants.

(F) Quantitation of the data shown in (E). The DNA bound fraction at  $[\text{HIRAN}] = 0 \mu\text{M}$  is not plotted.

(G) Dissociation constants ( $K_d$ ) extracted from the binding isotherms shown in (F). Absolute  $K_d$  values for WT and F142A are approximations since the transition range was not defined, but are consistent with  $K_d$  values in Figure 2B. Values represent the average  $\pm$  SD of three independent measurements. See also Figure S3.

its activity using this as a substrate. Strikingly, the 3'-PO<sub>4</sub>-capped fork structure was efficiently reversed by SMARCAL1, and there was no difference in the ability of this enzyme to reverse the capped versus uncapped substrate (Figure 6B). Furthermore, fork regression by the DNA helicases RecG and UvsW was similarly unaffected by the 3'-PO<sub>4</sub>-capped fork structure (Figures S5B and S5C). Together, these findings suggest the requirement of the free 3' end of the nascent leading strand is specific to HLTF, and thus indicate there is a fundamental difference in how HLTF recognizes and reverses stalled forks as compared to SMARCAL1, UvsW, and RecG.

### The HIRAN Domain Is Necessary for HLTF to Slow Replication Forks upon dNTP Depletion

Next, we wanted to determine whether HLTF function is required for replication fork remodeling in cells, and the contribution of the HIRAN domain to this function. Nucleotide depletion induced by hydroxyurea (HU) is commonly used to disrupt fork progression in eukaryotic cells and has recently been shown to promote fork reversal (Zellweger et al., 2015). As HU would also expose the nascent 3' end of DNA, we reasoned that HLTF's fork reversal activity might be required under these conditions. To test this hypothesis, we monitored replication fork progression in the

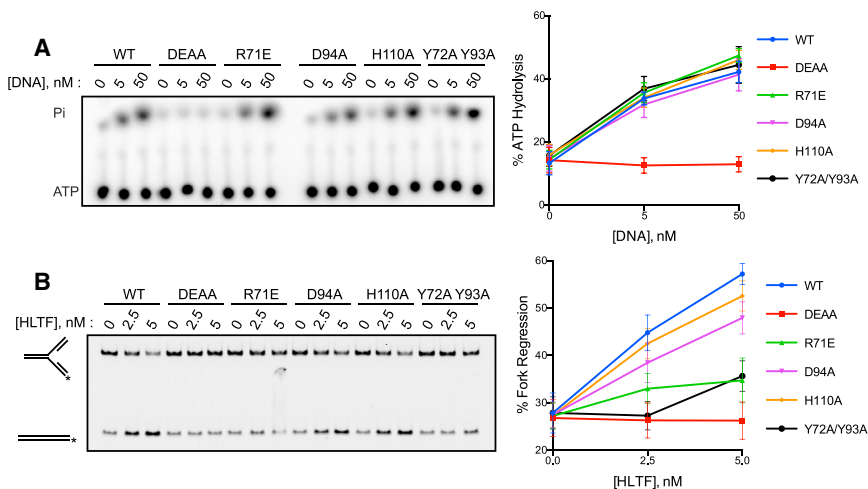


**Figure 5. HIRAN Is Necessary for Efficient DNA Fork Regression by HLTF**

(A) Left, representative ATPase activity of 50 nM WT versus ATPase-dead (DEAA) or HIRAN mutant HLTF proteins incubated with the indicated amount of splayed-arm DNA. Right, average values  $\pm$  SEM from triplicate experiments.

(B) Left, representative fork regression experiment of model DNA forks by the indicated amount of WT, ATPase-dead (DEAA), or HIRAN mutant HLTF proteins. The \* represents the position of the 5'-FAM-labeled 75-mer oligonucleotide in the fork structure and product. Right, quantification of the mean values  $\pm$  SEM from triplicate experiments. See also Figure S4.

presence of 50  $\mu$ M HU, a dose that reduces fork progression by approximately 45% as measured by fiber assay (Figure S6A) (Jackson and Pombo, 1998). To disrupt HLTF function, we knocked out the *HLTF* gene in U2OS cells (Figure 7A; Figures S6B–S6D). Using two *HLTF*-knockout lines and the parental line, we then monitored the effects of HLTF loss on replication fork progression using the fiber assay. We pulsed U2OS cells with IdU (30 min, red) followed by CldU (30 min, green) in the presence or absence of 50  $\mu$ M HU, and then measured CldU tracks (Figure 7B). Surprisingly, *HLTF*-knockout cells had substantially longer CldU tracks than did the parental cells in the presence of HU (Figures 7C and 7D). We obtained similar results upon siRNA-mediated knockdown of HLTF (Figure S6E). However, the knockout of *HLTF* had no effect in untreated cells (Figures 7C and 7D). These unexpected observations suggest that HLTF functions at the stalled replication fork to restrain replication fork progression, and are consistent with the idea that HLTF has a fork remodeling activity that slows fork progression under conditions of replication stress.

To determine if the fork progression phenotype is dependent on HLTF's HIRAN domain, we compared the ability of wild-type HLTF and the HIRAN mutants to rescue this phenotype in one of the *HLTF*-knockout lines. Expression of wild-type HLTF in the *HLTF*-knockout line restored the CldU track length to wild-type levels (Figure 7E). Next, we tested the HIRAN mutants that showed defective in vitro fork reversal activity in the fiber assay, as well as an ATPase mutant (Figure 7E). As expected, the ATPase mutant did not reduce the CldU track length. Strikingly, we also found that none of the HIRAN mutants tested could restore CldU track length to wild-type levels, despite the fact that they were expressed at levels similar to the wild-type HLTF. Thus, the HIRAN domain is necessary for HLTF's function at the replication fork. Taken together, these findings strongly suggest that HLTF constrains replication fork progression through HIRAN-mediated replication fork reversal.

## DISCUSSION

In this study, we present biochemical, structural, and biological evidence that the HIRAN domain of HLTF is a 3' ssDNA end-

binding module important for replication fork reversal and proper replication fork progression following replication stress. Several lines of data support these conclusions. First, the HIRAN domain of HLTF binds tightly and specifically to the 3' end of ssDNA. Second, residues lining the ssDNA binding pocket identified in the crystal structure of the HIRAN domain are critical for 3' end binding in solution. Third, the ability of HLTF to efficiently regress model replication forks is dependent on a functional HIRAN domain and a free 3'-hydroxyl group on the nascent leading strand of the model fork structure. Finally, the HIRAN domain is required for HLTF to restrain replication fork progression in vivo. These findings provide crucial insights into the mechanism of replication fork regression by HLTF, and suggest that HLTF helps maintain genome stability by promoting replication fork reversal following replication stress.

The HIRAN domain was first identified as an evolutionarily conserved domain of unknown function, but its location within proteins containing DNA-processing domains led to the prediction that it was needed to associate with damaged DNA or stalled replication forks (Iyer et al., 2006). However, thus far there has been no evidence to support this hypothesis. Our biochemical and structural data now show the HIRAN domain to be a bona fide DNA-binding domain with an unexpected 3' end binding activity that is essential for HLTF-dependent fork reversal. The strong structural similarity between human HLTF and *Lactobacillus* lp\_0118 (Figure S2C) HIRAN domains, and the conservation of the DNA binding residues in all of the known HIRAN sequences (Figure S1) imply that this 3' end binding activity is a universal feature of HIRAN-containing proteins across all kingdoms of life in which they appear. The HIRAN structure is adapted from an OB-fold, a general nucleic acid-binding motif most commonly associated with ssDNA binding, but also known to interact with a variety of ssDNA and dsDNA and RNA structures. To our knowledge, however, the specific interaction with the end of the DNA is unique to the HIRAN OB-fold.

Possibly the most revealing aspect of the structure and 3'-binding function of the HIRAN domain is its similarity to the PriA-3'BD. Both domains are coupled to a superfamily II type ATPase motor (Bhattacharyya et al., 2014), and capping the 3' end of the nascent leading strand in model fork structures

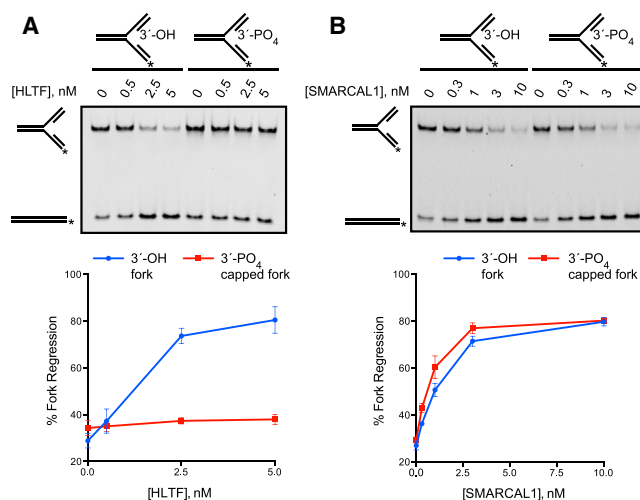


**Figure 6. Fork Regression by HLTF Is Promoted by the 3'-Hydroxyl End of the Leading Strand**

(A) Representative fork regression activity for HLTF on a model fork substrate with either a 3'-OH or a 3'-PO<sub>4</sub> end on the leading strand, with quantification below. A graph of mean values  $\pm$  SEM for three replicate experiments is shown.

(B) Fork regression experiments as in (A), but with the indicated amounts of SMARCAL1 and quantification below. A graph of mean values  $\pm$  SEM for three replicate experiments is shown. See also [Figure S5](#).

disrupts HLTF-mediated fork regression and PriA-fork binding (Mizukoshi et al., 2003). The PriA-3'BD is proposed to orient the protein at a stalled fork to enable the helicase domain to unwind the nascent lagging strand duplex and create the ssDNA necessary for reloading of DnaB helicase and the replication restart primosome (Gabbai and Marians, 2010; Jones and Nakai, 1999). In contrast, we propose that HLTF, which does not have strand-unwinding activity, combines its dsDNA translocase activity (Blastyák et al., 2010) with HIRAN's 3' end-binding function to recognize and reverse stalled forks (Figure 7F). We hypothesize that HLTF binds to dsDNA on the unreplicated template ahead of the replication fork, and uses its translocase activity to re-anneal the unwound template strands as it moves toward the stalled fork. Upon reaching the nascent leading strand, the translocase activity may destabilize the leading strand duplex allowing the HIRAN domain to capture the 3' ssDNA end. This would facilitate annealing of the nascent strands and formation of a four-way HJ. The translocase activity of HLTF would then promote branch migration and further fork reversal. In support of this 3'-capture model, our crystal structure and biochemistry show that HIRAN is not able to bind a duplexed 3' end.

Several additional lines of biochemical evidence support the proposed mechanism for fork reversal. First, HLTF binds dsDNA, a property that is likely associated with its SNF2 motor domain (Blastyák et al., 2010; Dürr et al., 2005; Singleton et al., 2007), and not its HIRAN domain. Furthermore, HLTF does not appear to have a preference for binding to different fork structures (Blastyák et al., 2010). Second, the ability of HLTF to reverse a model replication fork in vitro is significantly diminished when key DNA-binding residues in the HIRAN domain are mutated, indicating that the HIRAN domain is needed for its biochemical

activity. In contrast, the ATPase activity of HLTF is not affected by these mutations, indicating that ATPase activity is separable from 3' end binding. Finally, model replication forks in which the leading strand 3'-OH has been capped are poor substrates for HLTF.

The HIRAN domain of HLTF may be analogous to the N-terminal HARP domain of SMARCAL1 in that both act as substrate recognition domains (Bétous et al., 2012; Mason et al., 2014). However, differences in the HIRAN and HARP structures as well as our finding that HLTF, but not SMARCAL1, requires a free 3' end on the nascent leading strand during fork regression, suggest that these two translocases utilize different mechanisms to recognize and/or remodel their substrates. The HIRAN domain may direct HLTF to forks where the 3' end is exposed, whereas the HARP domains of SMARCAL1 likely promote fork reversal by recognizing a particular conformation of DNA at the branch point (Bétous et al., 2012; Mason et al., 2014). ZRANB3, another SWI/SNF2 translocase capable of fork reversal, also exhibits a substrate preference distinct from SMARCAL1, although the molecular basis of this preference is unknown (Bétous et al., 2013; Ciccia et al., 2012). These differences in substrate recognition could allow HLTF, SMARCAL1, and ZRANB3 to act on different types of stalled fork structures. By extension, these results may also indicate that many fork remodeling proteins exist in mammalian cells because forks stalled by distinct obstacles require several different modes of fork recognition and remodeling.

Our cellular data support an in vivo role for HLTF in promoting replication fork reversal. First, we show using iPond that HLTF and RAD18 associate specifically with nascent DNA in cells; a proteomic analysis utilizing a related approach also identified HLTF at replication forks (Alabert et al., 2014). These findings suggest that HLTF travels with the replication fork, which would enable it to respond rapidly to DNA damage or replication stress. Second, we also find that depletion or deletion of HLTF leads to longer replication tracts under conditions of replication stress (Figure 7D; Figure S6E). HU dramatically increases the frequency of replication fork reversal in cells, and a defect in fork reversal could account for the effect of HLTF depletion on fork progression in the presence of HU (Zellweger et al., 2015). Although it is possible that other fork remodeling processes could lead to this phenotype, two other factors needed for fork reversal, RAD51 and PARP, are also required to slow the fork under conditions of genotoxic stress (Zellweger et al., 2015). More importantly, the fork progression phenotype we observe is dependent on the HIRAN domain, which is required for fork reversal in vitro. We therefore hypothesize that the increased fork speed observed upon loss of HLTF is a result of loss of fork reversal.

Our findings raise interesting questions about the role of the HIRAN domain and HLTF in the cell and how HLTF may function together with other DDT and fork reversal proteins. For example, the HIRAN domain could help recruit HLTF to the replication fork in cells, which consequently might impact the functions of other proteins. Indeed, although HLTF's role in promoting PCNA poly-ubiquitination is shared with other ligases (Krijger et al., 2011; Unk et al., 2010), a decrease in this modification brought about by HLTF loss could reduce the recruitment of ZRANB3, which

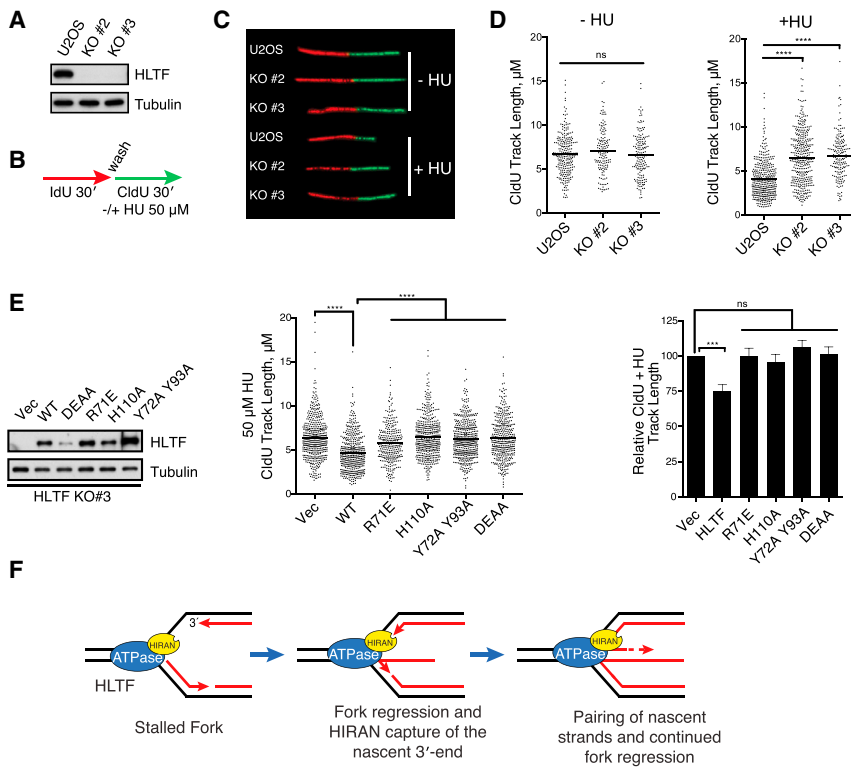


**Figure 7. Loss of HLTf Leads to Longer DNA Replication Tracks upon Depletion of Nucleotide Pools**

(A) Expression of HLTf in U2OS cells or CRISPR-generated *HLTF* knockout U2OS cells.

(B) Experimental setup. Cells were pulsed with IdU (30 min), then incubated with CldU and 50  $\mu$ M hydroxyurea (HU) for 30 min.

(C) Representative IdU and CldU replication tracks in WT U2OS and *HLTF*-knockout clones.

(D) Left, dot plot of CldU replication track lengths in the indicated cell lines. Right, dot plot of CldU replication tracks in the indicated cell lines after treatment with 50  $\mu$ M HU as in (B). In both experiments the line represents mean. \*\*\*\* $p < 0.0001$ , by two-tailed nonparametric Mann-Whitney test.

(E) Left, western blots of lysates from *HLTF* KO #3 cells transfected with empty vector (vec), WT, or mutant forms of HLTf. Middle, dot plot of CldU replication track lengths in *HLTF* KO #3 cells transfected as on the left and treated with HU as in (B). Line represents mean. \*\*\*\* $p < 0.0001$  was calculated using two-tailed nonparametric Mann-Whitney test. Right, relative CldU track lengths for  $n \geq 3$  replicates of the middle panel plotted  $\pm$  SEM, where vector-transfected cells are normalized to 100%.  $p = 0.0009$  was calculated using one-way ANOVA.

(F) Model of fork regression by HLTf, which utilizes the HIRAN domain to drive replication fork reversal. See also Figure S6.

associates with polyubiquitinated PCNA (Ciccia et al., 2012). It will also be important to determine how SMARCA1 and ZRANB3 affect fork progression under these conditions, and to investigate whether HLTf acts in the same pathway as these remodelers and as other proteins that restrain fork speed, such as RAD51 and PARP. Finally, the physiological effects of unrestrained replication fork progression are intriguing. HLTf's fork reversal activity may protect the replication fork and prevent the accumulation of mutations and genome instability. For instance, under conditions of nucleotide depletion, HLTf-mediated fork reversal could protect the fork by limiting ssDNA accumulation. Notably, *HLTF* is silenced in more than 40% of colon cancers, and its disruption promotes genome instability and intestinal carcinogenesis on the *Apc*<sup>min/+</sup> mutant background in mice (Sandhu et al., 2012; Unk et al., 2010). The Cancer Genome Atlas (TCGA) also indicates that *HLTF* amplification is observed in many cancers. We speculate that loss of HLTf could drive tumor progression by preventing a proper response to replication stress. Conversely, increased expression of HLTf may be advantageous in cancers that need to tolerate elevated levels of replication stress. HLTf may therefore be an important vulnerability point for tumorigenesis.

In summary, characterization of HLTf's HIRAN domain and elucidation of its DNA-bound structure reveal surprising clues about HLTf function and the mechanism of fork reversal, and could help pharmacological efforts to target HLTf activity in cancers. Moreover, the striking conservation of the ancient HIRAN domain throughout evolution and the role we have ascribed to it pave the way for functional studies on other uncharacterized HIRAN domain-containing proteins.

## EXPERIMENTAL PROCEDURES

Detailed procedures are available online in the [Supplemental Experimental Procedures](#).

### iPond

iPond was performed as previously described (Sirbu et al., 2011).

### Expression and Purification of Proteins

Cleavable His<sub>6</sub>-GST-*HLTF* proteins were expressed and purified from *S. cerevisiae* using tandem nickel and glutathione agarose chromatography. HIRAN domain proteins from human HLTf (amino acids 55–180) were expressed in *E. coli* and purified by nickel affinity followed by cleavage of the His<sub>6</sub>-GST-tag, heparin sepharose, and size exclusion chromatography.

### DNA Binding

The oligonucleotides used in EMSAs and DNA pull-downs are listed in Table S1. EMSAs were carried out at 25°C with 25 nM 6-carboxyfluorescein (FAM)-labeled oligonucleotides. Biotinylated oligonucleotides were incubated with the indicated protein for 1 hr at 4°C, washed, and boiled in sample buffer, then subjected to SDS-PAGE.

### HIRAN Crystallization and Structure Determination

The HLTf-HIRAN domain bound to dT<sub>10</sub> was crystallized by vapor diffusion, and the structure was determined by single isomorphous replacement with anomalous scattering phases from SeMet-substituted protein (Figure S2A; Table 1). The atomic model was refined and validated against native 1.5-Å diffraction data.

### NMR Spectroscopy of the HIRAN Domain

NMR structure calculations of the HLTf-HIRAN domain bound to dT<sub>10</sub> ssDNA were performed using CYANA based on NOE-derived distance, dihedral angle, and hydrogen bond restraints (Table S2). The 20 lowest-energy structures (of 200 total) were further refined in explicit solvent. For ssDNA versus

dsDNA binding measurements, <sup>15</sup>N-labeled HIRAN domain was gradually titrated with d(GCTGATAAAT) +/- its complementary strand. Chemical shift changes ( $\Delta\omega$ , Hz) were mapped onto the HIRAN structure by recording <sup>1</sup>H-<sup>15</sup>N HSQC spectra of the <sup>15</sup>N-HIRAN domain in the presence of a 2-fold excess of dT<sub>10</sub>.

### ATPase and Fork Regression Assays

ATPase- and oligonucleotide-based fork regression experiments were carried out as described (Blastyák et al., 2007, 2010), with minor modifications.

### Cell Culture, RNA Interference, and Plasmids

U2OS and HEK293T cells were maintained in DMEM (Life Technologies) supplemented with 10% FBS, 2 mM L-glutamine, and penicillin/streptomycin in 5% CO<sub>2</sub>, at 37°C. Plasmids and siRNA were transfected using Fugene6 (Promega) and Dharmafect 1 (Thermo Fisher Scientific), respectively, according to the manufacturer's directions.

### Reagents and Antibodies

$\gamma$ -tubulin (Sigma); IdU (BD Biosciences); CldU (BU1/75); SMARCA3/HLTF (Bethyl Laboratories); HLTF (Abcam); RAD18 (Novus Biologicals); PCNA (Santa Cruz Biotechnology); RPA70 (Bethyl Laboratories); and Histone H3 (Abcam) antibodies are all commercially available. The HLTF antibody was previously described (Lin et al., 2011). HU (Sigma), IdU (Fluka Chemical), and CldU (Sigma) are commercially available.

### CRISPR/Cas9-Mediated Knockout of HLTF in U2OS Cells

HLTF gene disruption was performed using the CRISPR/Cas9 system as described in Supplemental Experimental Procedures.

### DNA Fiber Experiments

U2OS and derivative cell lines were used to monitor DNA replication tracks essentially as described (Jackson and Pombo, 1998).

### ACCESSION NUMBERS

The accession number for the X-ray structure factors and coordinates reported in this paper is PDB: 4S0N, and the accession numbers for the NMR structure, chemical shift assignments, and restraints reported in this paper are PDB: 2MZN and BMRB: 25492. The accession numbers for the original diffraction images for native and SeMet derivative HIRAN-DNA crystals reported in this paper are SBGrid Databank: 129, 130.

### SUPPLEMENTAL INFORMATION

Supplemental Information includes six figures, two tables, and Supplemental Experimental Procedures and can be found with this article online at <http://dx.doi.org/10.1016/j.molcel.2015.05.013>.

### ACKNOWLEDGMENTS

This work was supported by an NIH grant (R01 ES016486) to K.A.C. and a grant from the Vanderbilt Center in Molecular Toxicology (P30 ES000267) to B.F.E. A.C.K. was funded by an American Cancer Society fellowship (PF-12-156-01-DMC) and an NIH training grant in Tumor Biology (T32 CA09151). D.A.C. was supported by the Vanderbilt Molecular Biophysics Training Program (NIH T32 GM08320). I.B. was supported by Regenerative Medicine Research Fund (#13-SCA-UCHC-03) and Connecticut Department of Public Health Biomedical Research Fund (#2013-0203). S.E. was supported by University of Connecticut Summer Undergraduate Research Fund (SURF). Use of the Advanced Photon Source at Argonne National Laboratory was supported by the US DOE under contract no. DE-AC02-06CH11357. Use of LS-CAT Sector 21 was supported by the Michigan Economic Development Corporation and the Michigan Technology Tri-Corridor (Grant 085P1000817). We thank David Cortez and Dan Jarosz for helpful discussions of the manuscript. We would also like to thank Briana Greer for help with biochemical assays and David Cortez for purified SMARCA1 protein.

Received: March 9, 2015

Revised: April 29, 2015

Accepted: May 1, 2015

Published: June 4, 2015

### REFERENCES

- Achar, Y.J., Balogh, D., and Haracska, L. (2011). Coordinated protein and DNA remodeling by human HLTF on stalled replication fork. *Proc. Natl. Acad. Sci. USA* *108*, 14073–14078.
- Alabert, C., Bukowski-Wills, J.-C., Lee, S.-B., Kustatscher, G., Nakamura, K., de Lima Alves, F., Menard, P., Mejlvang, J., Rappsilber, J., and Groth, A. (2014). Nascent chromatin capture proteomics determines chromatin dynamics during DNA replication and identifies unknown fork components. *Nat. Cell Biol.* *16*, 281–293.
- Bessho, Y., Shibata, R., Sekine, S., Murayama, K., Higashijima, K., Hori-Takemoto, C., Shirouzu, M., Kuramitsu, S., and Yokoyama, S. (2007). Structural basis for functional mimicry of long-variable-arm tRNA by transfer-messenger RNA. *Proc. Natl. Acad. Sci. USA* *104*, 8293–8298.
- Bétous, R., Mason, A.C., Rambo, R.P., Bansbach, C.E., Badu-Nkansah, A., Sirbu, B.M., Eichman, B.F., and Cortez, D. (2012). SMARCA1 catalyzes fork regression and Holliday junction migration to maintain genome stability during DNA replication. *Genes Dev.* *26*, 151–162.
- Bétous, R., Couch, F.B., Mason, A.C., Eichman, B.F., Manosas, M., and Cortez, D. (2013). Substrate-selective repair and restart of replication forks by DNA translocases. *Cell Rep.* *3*, 1958–1969.
- Bhattacharyya, B., George, N.P., Thurmes, T.M., Zhou, R., Jani, N., Wessel, S.R., Sandler, S.J., Ha, T., and Keck, J.L. (2014). Structural mechanisms of PriA-mediated DNA replication restart. *Proc. Natl. Acad. Sci. USA* *111*, 1373–1378.
- Blastyák, A., Pintér, L., Unk, I., Prakash, L., Prakash, S., and Haracska, L. (2007). Yeast Rad5 protein required for postreplication repair has a DNA helicase activity specific for replication fork regression. *Mol. Cell* *28*, 167–175.
- Blastyák, A., Hajdú, I., Unk, I., and Haracska, L. (2010). Role of double-stranded DNA translocase activity of human HLTF in replication of damaged DNA. *Mol. Cell. Biol.* *30*, 684–693.
- Branzei, D., and Foiani, M. (2010). Maintaining genome stability at the replication fork. *Nat. Rev. Mol. Cell Biol.* *11*, 208–219.
- Choi, K., Batke, S., Szakal, B., Lowther, J., Hao, F., Sarangi, P., Branzei, D., Ulrich, H.D., and Zhao, X. (2015). Concerted and differential actions of two enzymatic domains underlie Rad5 contributions to DNA damage tolerance. *Nucleic Acids Res.* *43*, 2666–2677.
- Ciccio, A., and Elledge, S.J. (2010). The DNA damage response: making it safe to play with knives. *Mol. Cell* *40*, 179–204.
- Ciccio, A., Nimmonkar, A.V., Hu, Y., Hajdu, I., Achar, Y.J., Izhar, L., Petit, S.A., Adamson, B., Yoon, J.C., Kowalczykowski, S.C., et al. (2012). Polyubiquitinated PCNA recruits the ZRANB3 translocase to maintain genomic integrity after replication stress. *Mol. Cell* *47*, 396–409.
- Ding, L., and Forsburg, S.L. (2014). Essential domains of *Schizosaccharomyces pombe* Rad8 required for DNA damage response. *G3 (Bethesda)* *4*, 1373–1384.
- Dong, G., Nowakowski, J., and Hoffman, D.W. (2002). Structure of small protein B: the protein component of the tmRNA-SmpB system for ribosome rescue. *EMBO J.* *21*, 1845–1854.
- Dürr, H., Kömer, C., Müller, M., Hickmann, V., and Hopfner, K.-P. (2005). X-ray structures of the *Sulfolobus solfataricus* SWI2/SNF2 ATPase core and its complex with DNA. *Cell* *121*, 363–373.
- Follonier, C., Oehler, J., Herrador, R., and Lopes, M. (2013). Friedreich's ataxia-associated GAA repeats induce replication-fork reversal and unusual molecular junctions. *Nat. Struct. Mol. Biol.* *20*, 486–494.
- Gabbai, C.B., and Marians, K.J. (2010). Recruitment to stalled replication forks of the PriA DNA helicase and replisome-loading activities is essential for survival. *DNA Repair (Amst.)* *9*, 202–209.

- Gangavarapu, V., Haracska, L., Unk, I., Johnson, R.E., Prakash, S., and Prakash, L. (2006). Mms2-Ubc13-dependent and -independent roles of Rad5 ubiquitin ligase in postreplication repair and translesion DNA synthesis in *Saccharomyces cerevisiae*. *Mol. Cell. Biol.* **26**, 7783–7790.
- Hishiki, A., Hara, K., Ikegaya, Y., Yokoyama, H., Shimizu, T., Sato, M., and Hashimoto, H. (2015). Structure of a novel DNA-binding domain of helicase-like transcription factor (HLTF) and its functional implication in DNA damage tolerance. *J. Biol. Chem.* Published online April 9, 2015. <http://dx.doi.org/10.1074/jbc.M115.643643>.
- Hoege, C., Pfander, B., Moldovan, G.L., Pyrowolakis, G., and Jentsch, S. (2002). RAD6-dependent DNA repair is linked to modification of PCNA by ubiquitin and SUMO. *Nature* **419**, 135–141.
- Iyer, L.M., Babu, M.M., and Aravind, L. (2006). The HIRAN domain and recruitment of chromatin remodeling and repair activities to damaged DNA. *Cell Cycle* **5**, 775–782.
- Jackson, D.A., and Pombo, A. (1998). Replicon clusters are stable units of chromosome structure: evidence that nuclear organization contributes to the efficient activation and propagation of S phase in human cells. *J. Cell Biol.* **140**, 1285–1295.
- Jones, J.M., and Nakai, H. (1999). Duplex opening by primosome protein PriA for replisome assembly on a recombination intermediate. *J. Mol. Biol.* **289**, 503–516.
- Krijger, P.H.L., Lee, K.-Y., Wit, N., van den Berk, P.C.M., Wu, X., Roest, H.P., Maas, A., Ding, H., Hoeijmakers, J.H.J., Myung, K., and Jacobs, H. (2011). HLTF and SHPRH are not essential for PCNA polyubiquitination, survival and somatic hypermutation: existence of an alternative E3 ligase. *DNA Repair (Amst.)* **10**, 438–444.
- Lin, J.-R., Zeman, M.K., Chen, J.-Y., Yee, M.-C., and Cimprich, K.A. (2011). SHPRH and HLTF act in a damage-specific manner to coordinate different forms of postreplication repair and prevent mutagenesis. *Mol. Cell* **42**, 237–249.
- Ma, J.-B., Ye, K., and Patel, D.J. (2004). Structural basis for overhang-specific small interfering RNA recognition by the PAZ domain. *Nature* **429**, 318–322.
- Mason, A.C., Rambo, R.P., Greer, B., Pritchett, M., Tainer, J.A., Cortez, D., and Eichman, B.F. (2014). A structure-specific nucleic acid-binding domain conserved among DNA repair proteins. *Proc. Natl. Acad. Sci. USA* **111**, 7618–7623.
- Minca, E.C., and Kowalski, D. (2010). Multiple Rad5 activities mediate sister chromatid recombination to bypass DNA damage at stalled replication forks. *Mol. Cell* **38**, 649–661.
- Mizukoshi, T., Tanaka, T., Arai, K., Kohda, D., and Masai, H. (2003). A critical role of the 3' terminus of nascent DNA chains in recognition of stalled replication forks. *J. Biol. Chem.* **278**, 42234–42239.
- Motegi, A., Sood, R., Moinova, H., Markowitz, S.D., Liu, P.P., and Myung, K. (2006). Human SHPRH suppresses genomic instability through proliferating cell nuclear antigen polyubiquitination. *J. Cell Biol.* **175**, 703–708.
- Motegi, A., Liaw, H.-J., Lee, K.-Y., Roest, H.P., Maas, A., Wu, X., Moinova, H., Markowitz, S.D., Ding, H., Hoeijmakers, J.H.J., and Myung, K. (2008). Polyubiquitination of proliferating cell nuclear antigen by HLTF and SHPRH prevents genomic instability from stalled replication forks. *Proc. Natl. Acad. Sci. USA* **105**, 12411–12416.
- Neelsen, K.J., and Lopes, M. (2015). Replication fork reversal in eukaryotes: from dead end to dynamic response. *Nat. Rev. Mol. Cell Biol.* **16**, 207–220.
- Neelsen, K.J., Zanini, I.M.Y., Herrador, R., and Lopes, M. (2013). Oncogenes induce genotoxic stress by mitotic processing of unusual replication intermediates. *J. Cell Biol.* **200**, 699–708.
- Ortiz-Bazán, M.Á., Gallo-Fernández, M., Saugar, I., Jiménez-Martín, A., Vázquez, M.V., and Tercero, J.A. (2014). Rad5 plays a major role in the cellular response to DNA damage during chromosome replication. *Cell Rep.* **9**, 460–468.
- Sandhu, S., Wu, X., Nabi, Z., Rastegar, M., Kung, S., Mai, S., and Ding, H. (2012). Loss of HLTF function promotes intestinal carcinogenesis. *Mol. Cancer* **11**, 18.
- Sasaki, K., Ose, T., Okamoto, N., Maenaka, K., Tanaka, T., Masai, H., Saito, M., Shirai, T., and Kohda, D. (2007). Structural basis of the 3'-end recognition of a leading strand in stalled replication forks by PriA. *EMBO J.* **26**, 2584–2593.
- Saugar, I., Ortiz-Bazán, M.Á., and Tercero, J.A. (2014). Tolerating DNA damage during eukaryotic chromosome replication. *Exp. Cell Res.* **329**, 170–177.
- Singleton, M.R., Dillingham, M.S., and Wigley, D.B. (2007). Structure and mechanism of helicases and nucleic acid translocases. *Annu. Rev. Biochem.* **76**, 23–50.
- Sirbu, B.M., Couch, F.B., Feigerle, J.T., Bhaskara, S., Hiebert, S.W., and Cortez, D. (2011). Analysis of protein dynamics at active, stalled, and collapsed replication forks. *Genes Dev.* **25**, 1320–1327.
- Theobald, D.L., Mitton-Fry, R.M., and Wuttke, D.S. (2003). Nucleic acid recognition by OB-fold proteins. *Annu. Rev. Biophys. Biomol. Struct.* **32**, 115–133.
- Tsutakawa, S.E., Classen, S., Chapados, B.R., Arvai, A.S., Finger, L.D., Guenther, G., Tomlinson, C.G., Thompson, P., Sarker, A.H., Shen, B., et al. (2011). Human flap endonuclease structures, DNA double-base flipping, and a unified understanding of the FEN1 superfamily. *Cell* **145**, 198–211.
- Unk, I., Hajdú, I., Fátyol, K., Szakál, B., Blastyák, A., Bermudez, V., Hurwitz, J., Prakash, L., Prakash, S., and Haracska, L. (2006). Human SHPRH is a ubiquitin ligase for Mms2-Ubc13-dependent polyubiquitylation of proliferating cell nuclear antigen. *Proc. Natl. Acad. Sci. USA* **103**, 18107–18112.
- Unk, I., Hajdú, I., Fátyol, K., Hurwitz, J., Yoon, J.-H., Prakash, L., Prakash, S., and Haracska, L. (2008). Human HLTF functions as a ubiquitin ligase for proliferating cell nuclear antigen polyubiquitination. *Proc. Natl. Acad. Sci. USA* **105**, 3768–3773.
- Unk, I., Hajdú, I., Blastyák, A., and Haracska, L. (2010). Role of yeast Rad5 and its human orthologs, HLTF and SHPRH in DNA damage tolerance. *DNA Repair (Amst.)* **9**, 257–267.
- Zellweger, R., Dalcher, D., Mutreja, K., Berti, M., Schmid, J.A., Herrador, R., Vindigni, A., and Lopes, M. (2015). Rad51-mediated replication fork reversal is a global response to genotoxic treatments in human cells. *J. Cell Biol.* **208**, 563–579.
- Zeman, M.K., and Cimprich, K.A. (2014). Causes and consequences of replication stress. *Nat. Cell Biol.* **16**, 2–9.